



**HAL**  
open science

# Tendon-Driven vs Rod-Driven Continuum Robots: A Bench Test Evaluation

Camille Benoist, Cédric Girerd, Nabil Zemiti, Philippe Poignet, Pierre Berthet-Rayne

► **To cite this version:**

Camille Benoist, Cédric Girerd, Nabil Zemiti, Philippe Poignet, Pierre Berthet-Rayne. Tendon-Driven vs Rod-Driven Continuum Robots: A Bench Test Evaluation. CRAS 2024 - Conference on New Technologies for Computer and Robot Assisted Surgery, Sep 2024, Odense, Denmark. hal-04690807v2

**HAL Id: hal-04690807**

**<https://hal.science/hal-04690807v2>**

Submitted on 10 Sep 2024

**HAL** is a multi-disciplinary open access archive for the deposit and dissemination of scientific research documents, whether they are published or not. The documents may come from teaching and research institutions in France or abroad, or from public or private research centers.

L'archive ouverte pluridisciplinaire **HAL**, est destinée au dépôt et à la diffusion de documents scientifiques de niveau recherche, publiés ou non, émanant des établissements d'enseignement et de recherche français ou étrangers, des laboratoires publics ou privés.

# Tendon-Driven vs Rod-Driven Continuum Robots: A Bench Test Evaluation

Camille Benoist<sup>1,2</sup>, Cédric Girerd<sup>1</sup>, Nabil Zemiti<sup>1</sup>, Philippe Pognet<sup>1</sup>, and Pierre Berthet-Rayne<sup>2,3</sup>

<sup>1</sup>LIRMM, Univ Montpellier, CNRS, Montpellier, France

<sup>2</sup>Caranx Medical - Nice, France

<sup>3</sup>3IA - Nice, France

camille.benoist@caranx-medical.com

## INTRODUCTION

Endoscopic robots are revolutionizing minimally-invasive surgery, by providing better standards of care for patients. They usually include a tubular system comprising a flexible passive proximal section and an active distal section, as illustrated in Fig. 1a. The distal section can bend continuously along its length, forming an equivalent structure of infinite number of joints with zero link length, referred to as a continuum robot (CR). The impact of CRs on the medical field is increasing thanks to their small size, high dexterity, flexibility, accuracy, and capacity to deploy along complex paths [1].

Tendon-driven robots are a particular type of CR, composed by a set of tendons routed along a flexible backbone. The actuation is performed by pulling and releasing the tendons, leading to backbone deflection. In order to increase the space available for tools while maintaining bending performance, notched tubes with tendons integrated in their walls have been proposed [2]. However, they can be subject to axial compression during actuation, which impairs their performance. To solve this challenge, the use of more rigid materials for the notched tube has been proposed, as well as the integration of additional backbones for structural support [2]. Nevertheless, these solutions decrease the bending performance and the space available for tools.

In this paper, a proposed design combines 3D printed flexible notched tubes with rods routed in their wall. The flexible notched tube enables large space for tools and preserves the bending performance, while the rods provide axial stiffness and enables pushing motions. This limits the axial compression experienced with tendon-driven robots and allows for more precise control of the robot length.

## MATERIALS AND METHODS

### A. Design Requirements

Following discussions with clinicians, a robot for flexible endoscopy in the stomach should be able to bend in all directions, with a bending angle ranging from 0 to 180°. It should have a minimum bending section length of 80 mm, to enable visualization of all regions within the stomach. In addition, its external diameter must be lower than 18 mm to enable safe navigation in the esophagus and the stomach, and it must accommodate multiple channels for sensors, air, water and surgical tools [2].

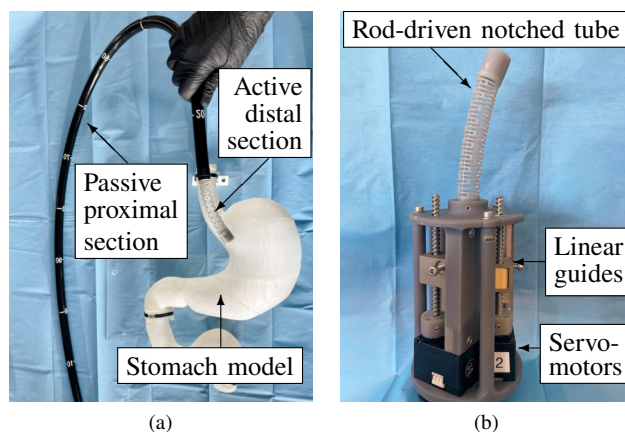


Fig. 1: (a) Photo of the proposed flexible endoscopic robot concept, and (b) photo of the proposed rod-driven notched tube robot prototype.

### B. Notched Tube Design and Fabrication

In agreement with the design requirements, the proposed notched tube forming the bending section is designed with an outer diameter of 14 mm and an inner diameter of 11 mm. Its overall length is 80 mm, with a 70 mm bending section and a 10 mm straight distal section for tool attachment. The bending section comprises a set of 3 symmetrical notches as represented in Fig. 2a, similar to [3], able to withstand large deformations. They are repeated 10 times along the robot length, as visible in Fig. 2b. Each set of 3 symmetrical notches is obtained by stacking and rotating one initial notch by 120°. Each notch serves as a flexible hinge, enabling rotation around one axis. The combination of 3 notches thus enables 3-DOF motions. Three channels of diameter 0.8 mm, evenly spaced by 120° around the tube centerline, are created inside the tube wall to accommodate 0.5 mm

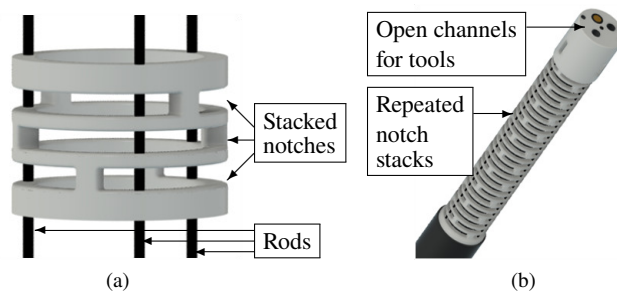


Fig. 2: (a) Representation of the set of 3 notches, repeated along the bending section of the tube, with the embedded rods. The entire notched tube is represented in (b).

diameter stainless steel rods for the actuation (see Fig. 2a). A Formlabs printer (Formlabs, Somerville, USA) is used with the flexible and biocompatible Tough 1500 Resin (Young’s modulus of 1.4 GPa) to fabricate the notched tube.

### C. Actuation System

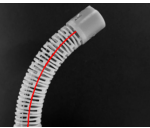
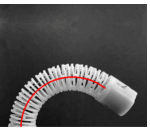
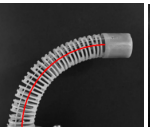
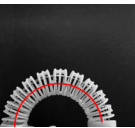
The proposed design requires rod translations to deflect the notched tube. They are performed by three actuators (Dynamixel XL330 servomotors, ROBOTIS, Seoul, Korea) via three linear guides at the device base. The fabricated prototype is visible in Fig. 1b. Similarly, a tendon-driven actuation system was fabricated, to pull and release tendons in place of rods via capstans, for comparative study.

## RESULTS

### A. Tendon Driven vs Rod-Driven Robot: Comparison

Experiments were conducted to evaluate the performance of the proposed rod-driven robot prototype compared to its tendon-driven counterpart. For this purpose, each tendon and rod-driven robot was controlled to bend five times by the desired angles  $\theta_{des} = 90^\circ$  and  $180^\circ$ , while maintaining a length  $l_{des} = 70$  mm. A kinematic model with constant-curvature assumption was used to compute the required tendon/rod displacements with the relationship  $\Delta l_i = \frac{1}{\theta} l d \cos(\Phi_i)$  with the robot bending angle  $\theta$ , the tube length  $l$ , the tendon/rod routing radius  $d$ , and the angle  $\Phi_i$  between the robot’s bending direction and the angular location of tendon/rod  $i$  [4]. The deformed centerline of the robots were extracted using OpenCV. The mean bending

TABLE I: Deformed tendon-driven and rod-driven robot shapes for commanded bending angle of  $90^\circ$  and  $180^\circ$ , with estimated bending angles and backbone length reported.

| Tendon-driven robot   |   | Rod-driven robot  |   |
|---|---|---|---|
| $\theta_{des} = 90.0^\circ$   | $\theta_{des} = 180.0^\circ$  | $\theta_{des} = 90.0^\circ$   | $\theta_{des} = 180.0^\circ$  |
| $l_{des} = 70.0$ mm   | $l_{des} = 70.0$ mm   | $l_{des} = 70.0$ mm   | $l_{des} = 70.0$ mm   |
|  |  |  |  |
| $\theta_m = 69.5^\circ$   | $\theta_m = 134.6^\circ$  | $\theta_m = 90.0^\circ$   | $\theta_m = 180.1^\circ$  |
| $\theta_{mae} = 20.5^\circ$   | $\theta_{mae} = 45.4^\circ$   | $\theta_{mae} = 0.0^\circ$  | $\theta_{mae} = 0.1^\circ$  |
| $l_m = 65.2$ mm   | $l_m = 61.3$ mm   | $l_m = 70.3$ mm   | $l_m = 70.9$ mm   |
| $l_{mae} = 4.8$ mm  | $l_{mae} = 8.7$ mm  | $l_{mae} = 0.3$ mm  | $l_{mae} = 0.9$ mm  |

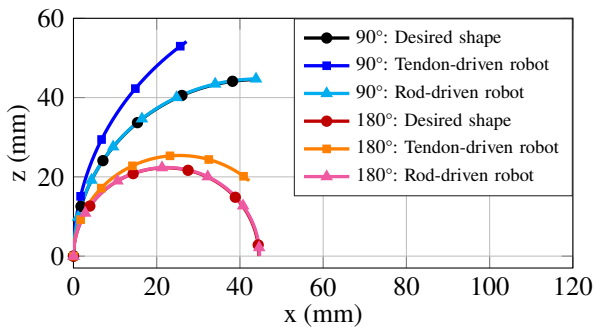
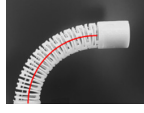
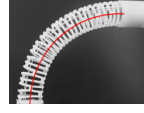

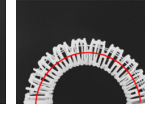


Fig. 3: Plot of the mean tendon-driven and rod-driven robot centerlines, and expected shapes from the kinematic model. The tendon-driven robot exhibits larger mean errors compared to the rod-driven robot.

TABLE II: Deformed rod-driven robot shapes with backbone compression and elongation, while keeping tip angles of  $90^\circ$  and  $180^\circ$ .

| Rod-driven robot  |  |   |   |
|---|--|---|---|
| $\theta_{des} = 90.0^\circ$   |  | $\theta_{des} = 180.0^\circ$  |   |
| $l_{des} = 60.0$ mm   | $l_{des} = 80.0$ mm  | $l_{des} = 60.0$ mm   | $l_{des} = 80.0$ mm   |
|  |  |  |  |
| $\theta_m = 90.9^\circ$   | $\theta_m = 90.7^\circ$  | $\theta_m = 178.6^\circ$  | $\theta_m = 179.0^\circ$  |
| $\theta_{mae} = 0.9^\circ$  | $\theta_{mae} = 0.7^\circ$   | $\theta_{mae} = 1.4^\circ$  | $\theta_{mae} = 1.0^\circ$  |
| $l_m = 59.9$ mm   | $l_m = 79.8$ mm  | $l_m = 60.1$ mm   | $l_m = 79.7$ mm   |
| $l_{mae} = 0.1$ mm  | $l_{mae} = 0.2$ mm   | $l_{mae} = 0.1$ mm  | $l_{mae} = 0.3$ mm  |

angles  $\theta_m$  and lengths  $l_m$ , as well as their mean absolute errors  $\theta_{mae}$  and  $l_{mae}$ , were then computed. Representative tendon and rod-driven robot shapes are visible in Table I, with the mean shapes plotted in Fig. 3. Overall, the tendon-driven robot shows larger errors for both bending angle and length compared to the rod-driven robot. This is related to compression of its backbone due to the lack of axial support. The rod-driven robot better matches the kinematic model thanks to the use of the rods, which enable more accurate control of the robot length. Moreover, additional positive outcomes were observed by using rods instead of tendons. They include more similar delays in the loading and unloading phases, and more repeatable returns to the straight configuration.

### B. Additional Rod-Driven Robot Capabilities

The precise control of the robot length by the rods also enables deliberate compression and extension of its backbone. An example is provided in Table II, where different robot lengths  $l_{des} = 60$  mm and  $80$  mm are selected, while maintaining robot tip angles of  $90^\circ$  and  $180^\circ$ . This capability of the robot further increases its workspace, and provides additional dexterity and reachability.

## CONCLUSIONS AND DISCUSSION

In this paper, a new rod-driven notched tube robot design was proposed. The design enables a large central lumen for tools, while enabling better control of the robot bending angle and length. It leads to decreased shape errors and better performance compared to a tendon-driven approach, and provides a larger variety of possible shapes by controlling the robot backbone length. Future work will focus on extending our rod-driven robot to multiple sections, and on the translation to medical applications.

## REFERENCES

- [1] J. Burgner-Kahrs, D. C. Rucker, and H. Choset, “Continuum robots for medical applications: A survey,” *IEEE Transactions on Robotics*, vol. 31, no. 6, pp. 1261–1280, 2015.
- [2] D. Song, S. Wang, Z. Zhang, X. Yu, and C. Shi, “A novel continuum overtube with improved triangulation for flexible robotic endoscopy,” *IEEE Transactions on Medical Robotics and Bionics*, 2023.
- [3] W. Zeng, J. Yan, K. Yan, X. Huang, X. Wang, and S. S. Cheng, “Modeling a symmetrically-notched continuum neurosurgical robot with non-constant curvature and superelastic property,” *IEEE Robotics and Automation Letters*, vol. 6, no. 4, pp. 6489–6496, 2021.
- [4] I. Robert J. Webster and B. A. Jones, “Design and kinematic modeling of constant curvature continuum robots: A review,” *The International Journal of Robotics Research*, vol. 29, no. 13, pp. 1661–1683, 2010.